ICES Journal of Marine Science, 58: 123–136. 2001
doi:10.1006/jmsc.2000.0996, available online at http://www.idealibrary.com on IDEAL®

Effects of *in situ* target spatial distributions on acoustic density estimates

J. Michael Jech and John K. Horne

Jech, J. M., and Horne, J. K. 2001. Effects of *in situ* target spatial distributions on acoustic density estimates. – ICES Journal of Marine Science, 58: 123–136.

One goal of acoustic-based abundance estimates is to accurately preserve spatial distributions of organism density and size within survey data. We simulated spatially-random and spatially-autocorrelated fish density and σ_{bs} distributions to quantify variance in density, abundance, and backscattering cross-sectional area estimates, and to examine the sensitivity of abundance estimates to organism spatial distributions and methods of estimating acoustic size. Our results show that it is difficult to simultaneously estimate fish density and maintain accurate σ_{bs}-frequency distributions. Among our acoustic backscatter estimation methods, a weighted-mean from a local search window provided optimal estimates of density, abundance and σ_{bs}. Other methods tended to bias either σ_{bs} or density estimates. This analysis identifies the relative importance of variance sources when estimating organism density using spatially-indexed acoustic data.

Key words: density estimates, spatial modeling, underwater acoustics.

Received 9 November 1998; accepted 13 November 2000.

J. M. Jech, and J. K. Horne: Cooperative Institute for Limnology and Ecosystem Research, University of Michigan, and NOAA-Great Lakes Environmental Research Laboratory, 2205 Commonwealth Blvd., Ann Arbor, MI 48105, USA. J. M. Jech: Present address: Northeast Fisheries Science Center, 166 Water St., Woods Hole, MA 02543, USA. J. K. Horne: Present address: University of Washington and NOAA Alaska Fisheries Science Center, 7600 Sand Point Way NE, Bldg. 4, Seattle, WA 98115, USA. Correspondence to J. M. Jech: tel: (508) 495 2353; fax: (508) 4952258; e-mail: michael.jech@noaa.gov

Introduction

Underwater acoustic technologies are non-invasive sampling tools commonly used to map distributions of fish and zooplankton abundance, density, and size. Advances in hardware and computing technology have increased the spatial resolution of acoustic data, thereby improving the ability to examine organism distributions at multiple scales (e.g. Horne and Schneider, 1997), to investigate predator–prey interactions (Levy, 1991), biological–physical interactions (Nash *et al*., 1989; Megard *et al*., 1997), or use in bioenergetic modeling (Luo and Brandt, 1993; Brandt and Mason, 1994). Goals of fisheries acoustics are to provide accurate abundance estimates and to preserve spatial distributions of organism densities and sizes within survey data.

Spatially-explicit analysis formalizes methods for extracting quantitative spatiotemporal information from acoustic data (Brandt *et al*., 1992; Mason and Brandt, 1996). Acoustic data are stored and analyzed in two-dimensional arrays where each array dimension is partitioned into cells to maintain the spatial heterogeneity observed in organism distributions. Each cell contains volume backscatter integrated over the dimensions of the cell [i.e. integrated echo (Dragesund and Olsen, 1965; Røttingen, 1976; Foote, 1978)] and backscattering cross-sectional areas (σ_{bs}) of individual targets. Assuming that backscatter from targets is incoherent and linearly additive (Foote, 1983), numeric density is the total energy returned from a sample volume, divided by the energy from a representative scatterer within that volume (Medwin and Clay, 1997).

$$\hat{\rho}_v = \frac{s_v}{\sigma_{bs}} \quad (1)$$

where $\hat{\rho}_v$ is the density estimate [number m^{-3}], s_v is vertically integrated and horizontally averaged volume backscatter over the spatial dimensions of the array cell, and $\hat{\sigma}_{bs}$ is the representative acoustic backscattering cross-sectional area (Figure 1).

1054–3139/01/010123+14 $35.00/0

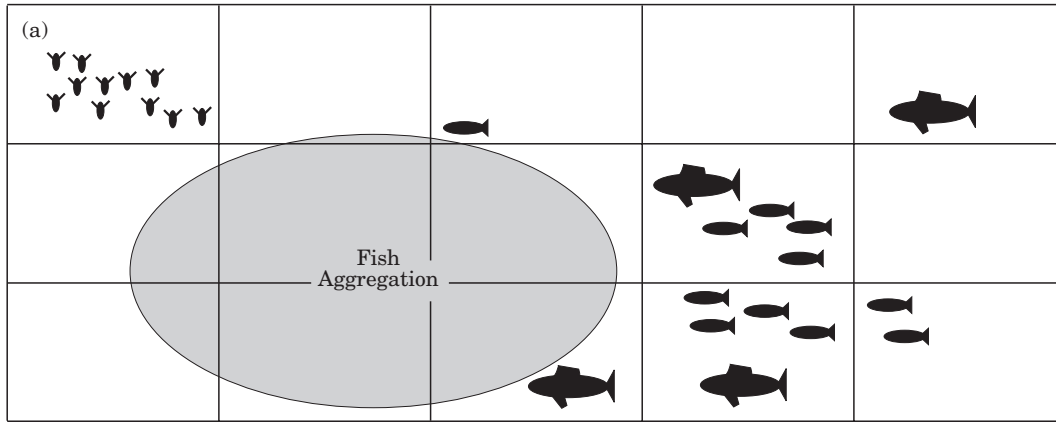

(b)				
$Sv = \Sigma\sigma_z$ $\hat{\rho} = Sv/\hat{\sigma}_z$	$Sv = \Sigma\sigma_?$ $\hat{\rho} = Sv/\hat{\sigma}$	$Sv = \Sigma\sigma_? + \Sigma\sigma_y$ $\hat{\rho} = Sv/\hat{\sigma}$	$Sv = 0$ $\rho = 0$	$Sv = \Sigma\sigma_p$ $\hat{\rho} = Sv/\hat{\sigma}_p$
$Sv = \Sigma\sigma_?$ $\hat{\rho} = Sv/\hat{\sigma}$	$Sv = \Sigma\sigma_?$ $\hat{\rho} = Sv/\hat{\sigma}$	$Sv = \Sigma\sigma_?$ $\hat{\rho} = Sv/\hat{\sigma}$	$Sv = \Sigma\sigma_y + \Sigma\sigma_p$ $\hat{\rho} = Sv/\hat{\sigma}$	$Sv = 0$ $\rho = 0$
$Sv = \Sigma\sigma_?$ $\hat{\rho} = Sv/\hat{\sigma}$	$Sv = \Sigma\sigma_?$ $\hat{\rho} = Sv/\hat{\sigma}$	$Sv = \Sigma\sigma_? + \Sigma\sigma_p$ $\hat{\rho} = Sv/\hat{\sigma}$	$Sv = \Sigma\sigma_y + \Sigma\sigma_p$ $\hat{\rho} = Sv/\hat{\sigma}$	$Sv = \Sigma\sigma_y$ $\hat{\rho} = Sv/\hat{\sigma}_y$

Figure 1. Acoustic echogram and corresponding spatially-indexed array. The top schematic (a) represents potential distributions of aquatic organisms observed along acoustic transects. Data array cells can contain resolved individuals of single or multiple species, no resolvable individual targets (i.e. fish aggregation), or may contain different species, sizes and scattering types. The bottom schematic (b) shows the corresponding spatially-indexed array. σ_p, σ_y, σ_z are acoustic backscattering cross-sections of predators, prey, and zooplankton, respectively. $\hat{\sigma}$, $\hat{\rho}$ are the estimated backscatter and estimated density, and s_v is volume scattering. $\sigma_?$ represents cells without resolvable individual targets. In cells with volume scattering and no resolved targets, a $\hat{\sigma}_{bs}$ must be estimated.

Selections of $\hat{\sigma}_{bs}$ are critical for accurate density estimates. Strategies to choose a representative acoustic backscattering cross-section can be grouped in two general categories: *in situ* targets, and acoustic–catch relationships. In this paper, we focus on utilizing *in situ* targets for calculating numeric density estimates within acoustic data array cells. *In situ* targets are acoustically resolved individuals using single- (Craig and Forbes, 1969), dual- (Ehrenberg and Torkelson, 1996) or split-beam (Foote *et al.*, 1986; Soule *et al.*, 1996; Demer *et al.*, 1999) hardware and analyses.

We simulated spatially-random and spatially-correlated fish density and backscattering strength distributions to examine the influence of spatial distribution, σ_{bs}-frequency distribution, and strategies used to estimate $\hat{\sigma}_{bs}$ on the accuracy of density and abundance estimates in spatially-indexed acoustic data using *in situ* targets. These simulations represent methods for interpolating backscattering cross-section estimates into sampling volumes where individual targets are not detected. It is important to note that we are not simulating techniques for reliable measures of individual targets, but investigating how to use *in situ* data for reliable estimates of organism density and abundance. Our specific questions are: does the σ_{bs}-frequency distribution of a fish population affect accuracy of density and abundance; does decreasing numbers of *in situ* targets affect accuracy of fish density and abundance estimates, and does the spatial distribution of fish density and backscattering strength affect accuracy of density and abundance estimates?

Materials and Methods

Simulated spatial distributions of fish densities and sizes were designed to reflect fish distributions commonly observed with underwater acoustics in a variety of freshwater and coastal ecosystems. Two discrete categories of spatially-correlated data were used in simulations: random and autocorrelated. Four spatial distributions were simulated (Table 1): (1) random-density and random-σ_{bs} (Random Distribution), (2) random-density and autocorrelated-σ_{bs} (Dispersal Layers), (3) autocorrelated-density and random-σ_{bs} (Mixed Aggregations), and (4) autocorrelated-density and autocorrelated-σ_{bs} (Discrete Aggregations). The Random Distribution simulates heterogeneous combinations of backscattering strengths within cells, where densities and σ_{bs}'s are independent among cells. Dispersed Layer simulations emulate a two layer distribution with a dominant fish size in each layer. This structure is analogous to two thermally segregated species. Mixed Aggregation simulations model crepuscular periods when different fish species and sizes co-occur. Discrete Aggregation simulations are potentially the most realistic, simulating patchy distributions of similar sized fish within each patch.

Array generation

All simulations use a 200 × 200 array (40 000 cells) with a known number of fish per cell (density), and a known length and σ_{bs} for each fish. To facilitate comparison among simulations and $\hat{\sigma}_{bs}$ estimation methods, fish abundances were kept as consistent as possible among simulations (Table 1). Four length-frequency distributions: normal unimodal, normal bimodal, Poisson unimodal, and Poisson bimodal were generated to populate the array (Figure 2). Mean and standard deviations of these length-frequency distributions (Table 1) were based on October 1996 survey data from Lake Ontario. Fish lengths were converted to σ_{bs} using an equation derived by Foote (1987), and the conversion from fish length to σ_{bs} is assumed to represent the "true" length-frequency distribution. Random selections were chosen using a pseudo-random number generator from IDL (Interactive Data Language, Research Systems Inc., Boulder, Colorado, USA).

Random distribution: spatially-random density and σ_{bs} distributions

Spatially-random distributions of fish densities and σ_{bs}'s for the Random Distribution simulation were obtained by randomly filling 79% of array cells with fish densities, fish lengths and corresponding backscattering cross-sections (upper left panel, Figure 3). Cell densities were randomly chosen from a Poisson distribution with the mean equal to 1.55. Resulting cell densities ranged from 0–10 fish per cell. Fish lengths were randomly chosen from the four length-frequency distributions depending on simulation (Table 1), converted to σ_{bs}, and then randomly placed in cells throughout the array.

Dispersed layer simulations: spatially-random density and spatially-autocorrelated σ_{bs} distributions

Spatially-random density distributions in Dispersed Layer simulations were chosen as in Random Distribution simulations. Spatially-autocorrelated σ_{bs} distributions were obtained by using only bimodal length-frequency distributions. In the upper portion of the array, fish lengths were randomly chosen from the smaller length-frequency mode to represent prey-sized fish. In the lower portion of the array, fish sizes were randomly chosen from the larger length mode to represent predator-sized fish (Figure 2).

Mixed aggregation simulations: spatially-autocorrelated density and spatially-random σ_{bs} distributions

Spatially-autocorrelated densities in Mixed Aggregation simulations were produced by kriging. Kriging is a statistical technique that estimates one- or two-dimensional covariances in spatially-indexed data (Cressie, 1991). Estimating spatial variance in fish distributions is an example of the forward approach for obtaining abundance estimates using acoustic transect data (e.g. Petitgas, 1993). We used an inverse approach (similar to Simmonds and Fryer, 1996) to produce a density map with specified variance and autocorrelation. A spherical variance model was used to krig fish densities with the parameter values: range=26, nugget=0, and sill=3 (Table 1). Patches are defined using the range parameter, where cells within a radius of 26 cells from the center cell are autocorrelated. The nugget parameter defines the amount of randomness in the data. The nugget was set to zero in Random Distribution and Dispersed Layer models to simulate random density distributions. The sill parameter defines variability within a patch. Center cells for 85 patches were randomly chosen, and an additional 150 cells along a single row were designated as a layer. Initial fish densities for each patch were randomly chosen from a Poisson distribution with a mean of 2.15 (0–8 fish per cell). A mean of 2.15 generated fish abundances similar to those used in random density simulations. Initial cell densities within the layer were set to the maximum density of eight fish per cell.

The array containing these initial patch and layer cells was kriged using the spherical model to produce an array with autocorrelated density structure (lower left

Table 1. Simulation parameters and variables. "Mean cell density" is the Poisson distribution mean used in each simulation.

Simulation	Spatial density distribution	Spatial length distribution	Length-frequency distribution	Mean length (mm)	Mean cell density (number cell^{-1})	Total abundance		
1. Random distribution	(a) Random	Random	Normal unimodal	140	1.55	62 096		
	(b) Random	Random	Normal bimodal	100, 160	1.55	62 096		
	(c) Random	Random	Poisson unimodal	140	1.55	62 096		
	(d) Random	Random	Poisson bimodal	90, 160	1.55	62 096		
2. Dispersed layers	(a) Random	Non-random	Normal bimodal	100, 160	1.55	62 096		
	(b) Random	Non-random	Poisson bimodal	90, 160	1.55	62 096		
3. Mixed aggregations	(a) Kriging	Random	Normal unimodal	140	2.15	61 123		
	(b) Kriging	Random	Normal bimodal	100, 160	2.15	61 123		
	(c) Kriging	Random	Poisson unimodal	140	2.15	61 123		
	(d) Kriging	Random	Poisson bimodal	90, 160	2.15	61 114		
4. Discrete aggregations	(a) Kriging	Non-random	Normal bimodal	100, 160	2.15	61 123		
	(b) Kriging	Non-random	Poisson bimodal	90, 160	2.15	61 108		
Total number of cells: 40 000		Random array numbers		Kriging model parameters		Kriged array numbers		
(200 × 200 grid)		Number filled	31 542	Model:	Spherical	Number high density cells	12 417	
		Number zero	8 458	Range:	26	Number low density cells	1 368	
				Nugget:	0	Number zero cells	26 215	
				Sill:	3	Number prey	58 387	3(a), (b), (c), 4(a)
							58 378	3(d)
							58 372	4(b)
						Number predators	2 736	

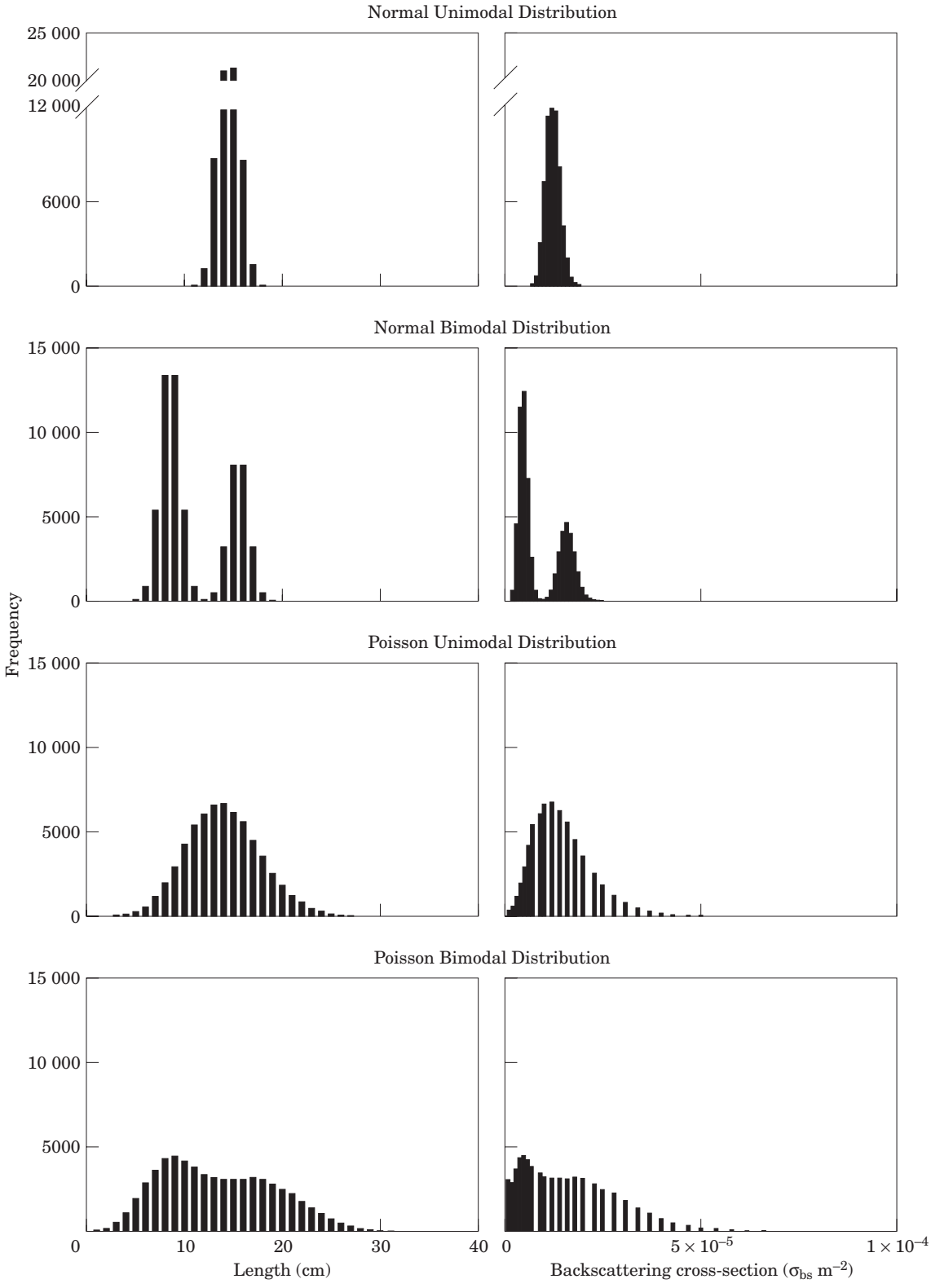

Figure 2. Length-frequency distributions of fish populations used in simulations. Bimodal distributions are formed by joining two unimodal distributions. Mean and standard deviations for each distribution are listed in Table 1.

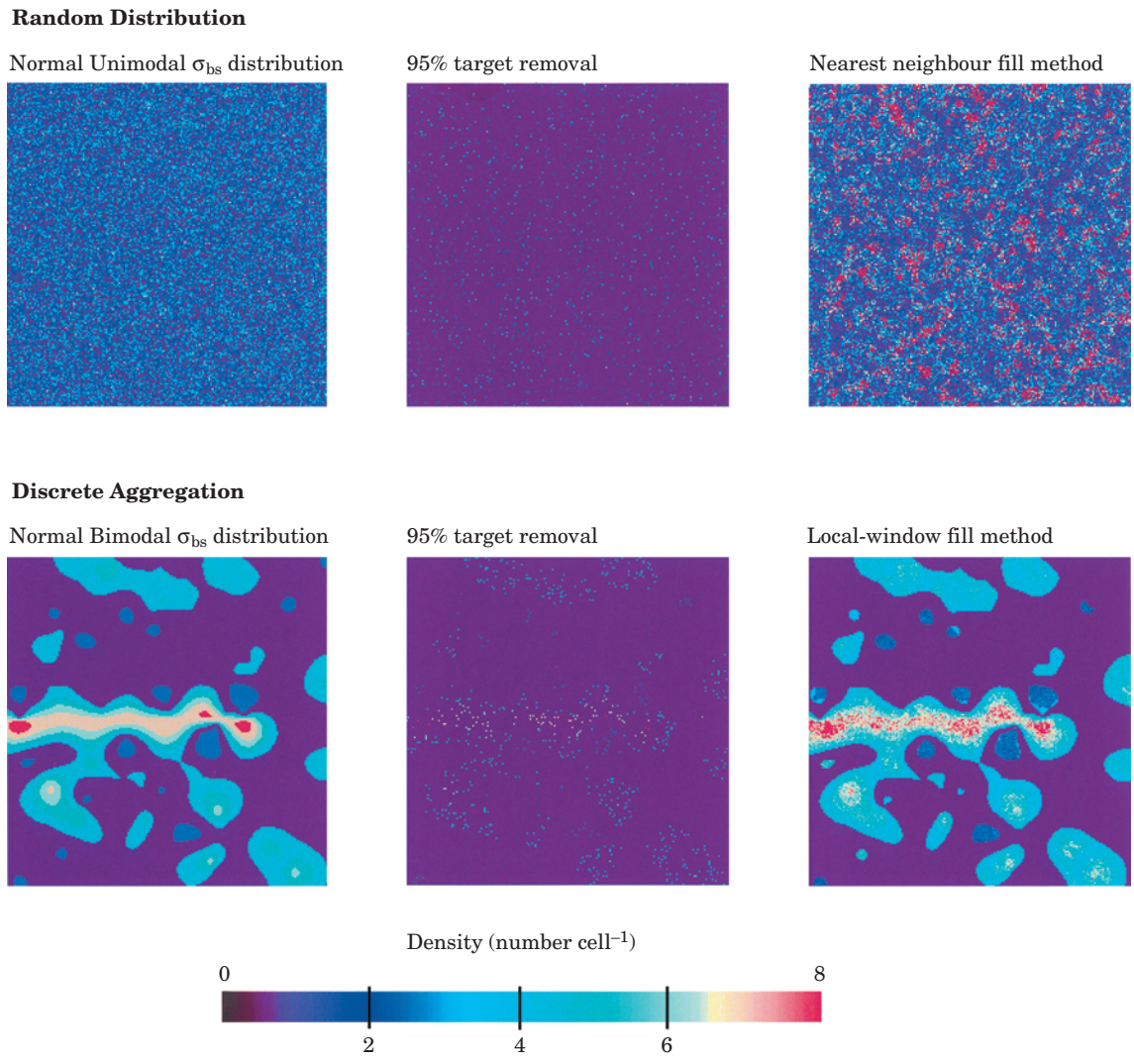

Figure 3. Density distribution arrays used in Random Distribution (random-density/random-length) and Discrete Aggregation (autocorrelated-density/autocorrelated-length) simulations. Arrays on the left show the original density distributions. Middle arrays show density distributions after 95% of the cells with targets are removed. Right-hand arrays show the distributions of estimated densities. The nearest-neighbor estimation method creates artificial spatial structure from random density distributions (upper right panel). The window-fill method preserved the original spatial density structure, even with low numbers of individual targets (lower right panel).

panel, Figure 3). To emphasize patch structure within the kriged array, patches were further categorized into high, low, and zero density. High-density patches were defined as cells with fish densities greater than the mean density of 2.15. Cell densities less than or equal to the mean and greater than or equal to zero were set to zero. Low-density patches were defined by setting cells with negative densities to a fish density of two.

In mixed aggregation simulations, fish lengths were randomly chosen from length-frequency distributions (Table 1), converted to σ_{bs}, and randomly placed in cells throughout the array, independent of patch density.

Discrete aggregation: spatially-autocorrelated density and σ_{bs} distributions

Spatially-autocorrelated fish density distributions were simulated using the same kriging process outlined in Mixed Aggregation simulations. Spatially-autocorrelated fish σ_{bs} distributions were obtained using only bimodal length-frequency distributions. Prey aggregations were simulated by placing smaller fish in high density patches and the layer. Isolated predators were simulated by placing larger fish in low density patches, and predator abundance was lower than in other simulations.

σ_{bs} estimation methods

Estimating density within array cells requires a representative $\hat{\sigma}_{bs}$ in each cell. Foote (1983) suggested that a weighted-mean backscattering cross-sectional area (σ_{bs}) be used as an estimate of $\hat{\sigma}_{bs}$ when targets within a sampling volume are of similar type (e.g. swimbladdered fish) and in sufficiently large numbers. In cells with one or more individual targets, a weighted-mean σ_{bs} of targets in each cell was used as the representative backscatter. In cells with no individual targets, but with non-zero volume scattering (e.g. fish aggregations with no resolvable targets), $\hat{\sigma}_{bs}$ was estimated using (1) a weighted-mean from the distribution of individual targets in the full array, (2) a weighted-random choice from the distribution of individual targets in the full array, (3) a weighted-mean from the distribution of targets within a local-search window, and (4) a nearest neighbor.

The weighted-mean estimation method uses a mean σ_{bs} from all individual targets throughout the array weighted by the frequency of occurrence. This mean backscatter is used as the representative $\hat{\sigma}_{bs}$ in all cells with non-zero volume backscattering but with no individual targets. The weighted-random estimation method chooses a representative backscatter from the distribution of all individual targets in the full array. Random choices are weighted by the frequency of occurrence and a new $\hat{\sigma}_{bs}$ is chosen for each cell. The local-window estimation method searches for individual targets by beginning with array elements immediately surrounding a cell, and then increases the search radius until either a minimum number of targets is found or a maximum window size is reached. Three window parameters: maximum window radius, window shape, and minimum number of targets define the search pattern and target criteria used to estimate a representative $\hat{\sigma}_{bs}$. We used a maximum radius of 25 cells, a symmetric (i.e. square) shape, and a minimum of five targets within the search window. Search patterns may be varied from symmetric to elongated shapes to accommodate different spatial distributions of organisms such as layers or patches. A minimum number of targets within the search window provides a distribution of targets for $\hat{\sigma}_{bs}$ estimation and avoids duplicating the nearest-neighbor search strategy. Setting a maximum window size restricts the search pattern to a local area where similar species are expected and avoids searching the entire array. When the minimum number of targets is found, the weighted-mean of those targets is used as the representative $\hat{\sigma}_{bs}$. If the maximum window size is reached and no individual targets are found, cell density is set to zero. Setting cell densities to zero is used as a diagnostic in the simulations. In practice, these cells can be set to another choice of $\hat{\sigma}_{bs}$. For the nearest-neighbor estimation method, the σ_{bs} of the nearest target is used as the representative $\hat{\sigma}_{bs}$. If two or more targets are equidistant, then the weighted-mean of those targets is used as the representative $\hat{\sigma}_{bs}$.

%Target removal

To simulate situations where individual targets are not resolved, all targets were removed from randomly chosen cells while retaining the known volume backscattering (%target removal). %target removal is calculated as the percentage of cells deleted from the array. It does not equal the percentage of individual targets removed, as a cell can contain more than one target. %target removal for each set of simulations was increased from 5% to 95% in 5% increments, and targets in remaining cells were used to estimate the representative $\hat{\sigma}_{bs}$ in cells lacking individual targets. The removal of targets from random cells did not modify the σ_{bs}-frequency distributions in any simulation. After estimating the backscattering cross-section within each cell, cell densities were computed using Equation (1) and fish abundance was calculated. Accuracy of fish density and abundance estimates was quantified by computing deviations between original (before target removal) and estimated data arrays.

Deviation indices were calculated as a function of %target removal to test the accuracy of each $\hat{\sigma}_{bs}$ estimation method. Accuracy of abundance estimates was quantified using a normalized abundance deviation index

$$\text{Abundance deviation index} = \frac{\sum_{i=1}^{Ncells} \hat{\rho}_i - \sum_{i=1}^{Ncells} \rho_{k_i}}{\sum_{i=1}^{Ncells} \rho_{k_i}} \tag{2}$$

where $\hat{\rho}$ is estimated density, ρ_k is known density in the i^{th} cell before target removal, and N_{cells} is the total number of cells in the array (40 000). Because initial fish abundances were not equal in all simulaitons (Table 1), abundance deviations were normalized to facilitate comparisons among simulations. Mean per-capita deviation indices for density and $\hat{\sigma}_{bs}$ estimates were computed using

$$\text{Density deviation index} = \frac{1}{N_{cells}} \sum_{i=1}^{Ncells} \left[\frac{\hat{\rho}_i - \rho_{k_i}}{\rho_{k_i}} \right] \tag{3}$$

$$\hat{\sigma}_{bs} \text{ deviation index} = \frac{1}{N_{cells}} \sum_{i=1}^{Ncells} \left[\frac{\hat{\sigma}_i - \sigma_{k_i}}{\sigma_{k_i}} \right] \tag{4}$$

where σ_k is the known backscattering cross-sectional area, and $\hat{\sigma}$ is the estimated value. The value of N_{cells} differs among abundance, density, and σ_{bs} deviation indices. For abundance deviation indices, N_{cells} is the number of cells in the array. For density and $\hat{\sigma}_{bs}$ indices,

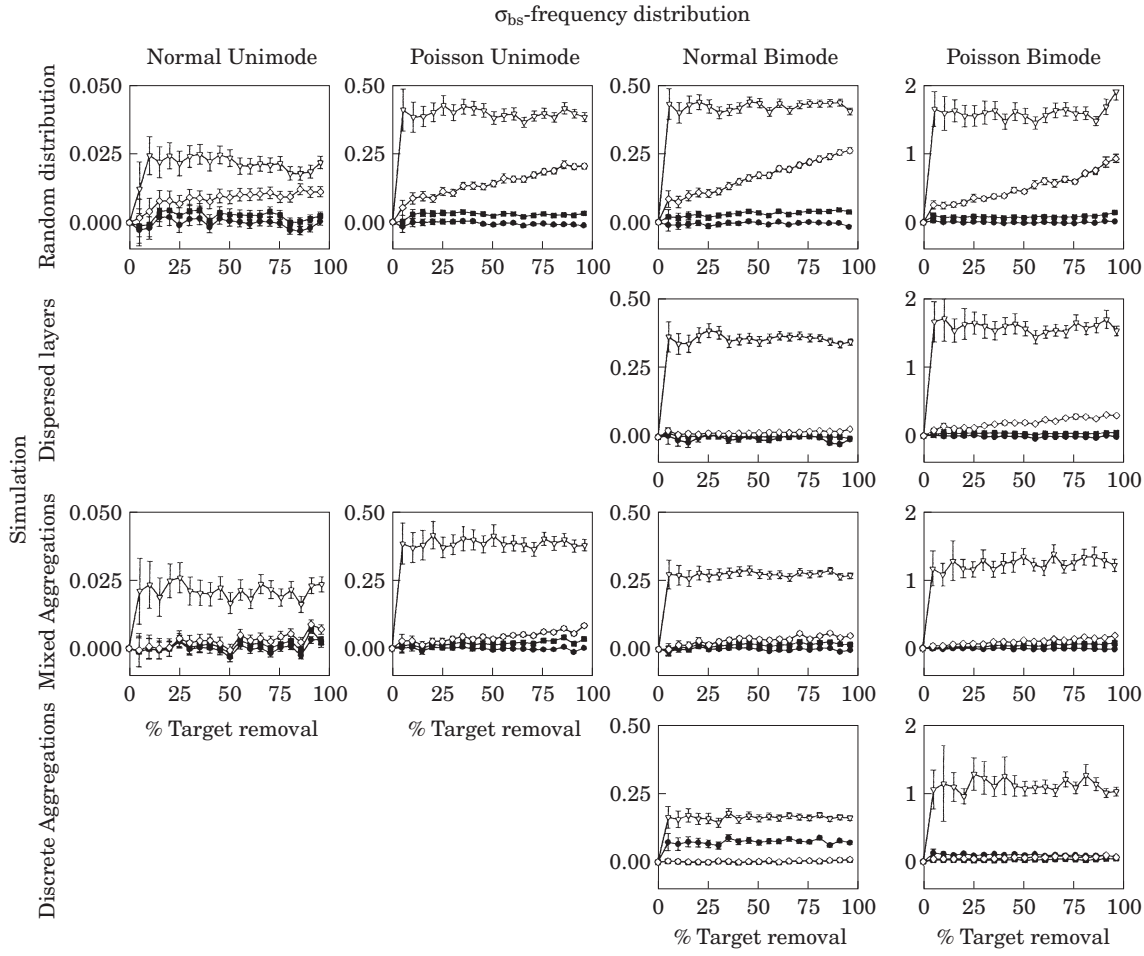

Figure 4. Mean per-capita density deviation index as a function of %target removal. %target removal was incremented in 5% steps. Column comparisons illustrate the effect of using different σ_{bs}-frequency distributions. Row comparisons illustrate the effect of using different $\hat{\sigma}_{bs}$ estimation methods on density estimates. $\hat{\sigma}_{bs}$ estimation methods are represented by: —●— mean fill, —▽— random fill, —■— local window, and —◇— nearest-neighbor.

N_{cells} is the number of cells with targets removed and N_{cells} increases as %target removal increases. Positive deviation index values indicate overestimates, whilst negative values indicate underestimates of fish density, abundance, and backscattering cross-sections. For abundance estimates, a deviation index value of 1 is equivalent to a doubling in abundance.

Results

Fish density, abundance, and $\hat{\sigma}_{bs}$ estimates were influenced by the choice of σ_{bs}-frequency distribution in all simulations (Figures 4–6). Density, abundance, and $\hat{\sigma}_{bs}$ estimates were most accurate using the normal unimodal distribution, whereas deviation indices were 1–2 orders of magnitude larger with the Poisson bimodal distribution. This reduced accuracy may result from the wider range of fish backscattering cross-sections in the Poisson distributions compared to the normal distributions. The local-window estimation method preserved spatial density structure in Discrete Aggregation simulations (bottom row Figure 3). The nearest-neighbor method created artificial structure from spatially random density distributions (top row Figure 3).

Estimates of fish density (Figure 4) and abundance (Figure 5) using the local-window method were consistently more accurate than other $\hat{\sigma}_{bs}$ estimation methods for all spatial distributions and σ_{bs}-frequency distributions. For all spatial distribution simulations and σ_{bs}-frequency distributions, the random-fill estimation method provided the least accurate density and abundance estimates (Figures 4 and 5). Using the nearest-neighbor method, density and abundance estimates were more accurate when density and σ_{bs} distributions were both spatially autocorrelated (Discrete Aggregations) than when spatial distributions were random (Figures 4

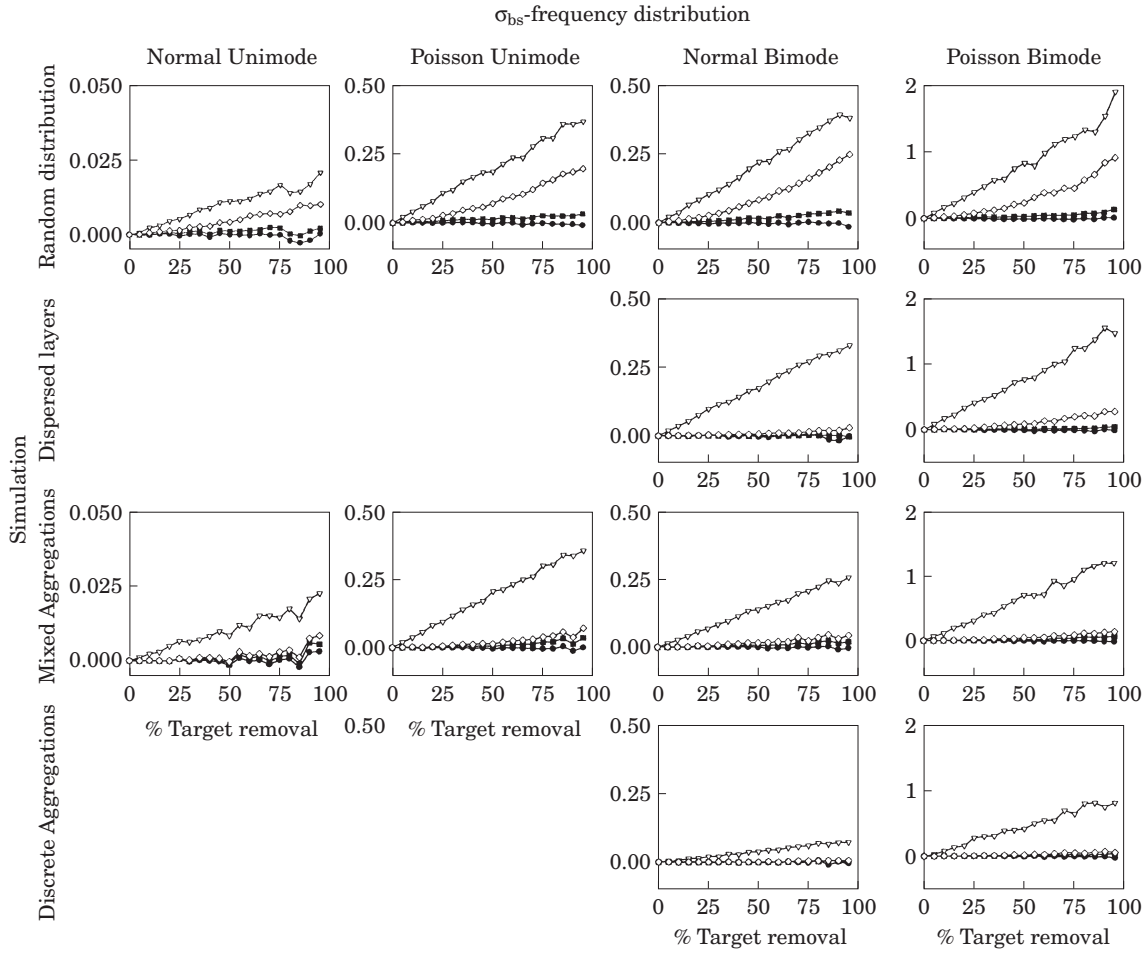

Figure 5. Abundance deviation index as a function of %target removal. %target removal was incremented in 5% steps. Column comparisons show the effect of using different σ_{bs}-frequency distributions, and row comparisons show the effect on abundance estimates using different $\hat{\sigma}_{bs}$ estimation methods. Estimation methods are represented by: —●— mean fill, —▽— random fill, —■— local window, and —◇— nearest-neighbor.

and 5). The mean-fill estimation method had density and abundance deviation index values near zero for Random Distribution, Dispersed Layer, and Mixed Aggregation simulations. For Discrete Aggregation simulations, density deviation values using the mean-fill method were higher than those using local-window and nearest-neighbor methods.

$\hat{\sigma}_{bs}$ deviation index values among all σ_{bs} estimation methods were similar for all simulation conditions except the Dispersed Layers simulation where deviation indices were near zero for the nearest-neighbour and window-fill methods (Figure 6). Although $\hat{\sigma}_{bs}$ deviation index values were similar, 95% confidence intervals were greatest for the random-fill method. The random-fill method was susceptible to choosing inappropriately small $\hat{\sigma}_{bs}$ values that resulted in exceptionally high density estimates. Although random choices were weighted by the frequency of occurrence, the random-fill method did not incorporate the spatial distribution of targets when estimating cell densities. When summing cell densities for population estimates, exceptionally high densities are not compensated by underestimated densities in other cells because the minimum density estimate in any cell is zero, and the maximum cell density is bounded by the smallest individual target.

Using a weighted mean backscattering cross-section in cells with resolved targets altered bimodal σ_{bs}-frequency distributions in simulations with spatially random distributions. In simulations with spatially autocorrelated backscattering cross-sections (Dispersed Layers and Discrete Aggregation simulations), distributions of σ_{bs} in cells with resolved targets replicated individual target σ_{bs}-distributions [vertical bars, Figure 7(b) and (d)]. When individual target sizes were spatially random (Random Distribution and Mixed Aggregation simulations), bimodal σ_{bs}-distributions from array cells

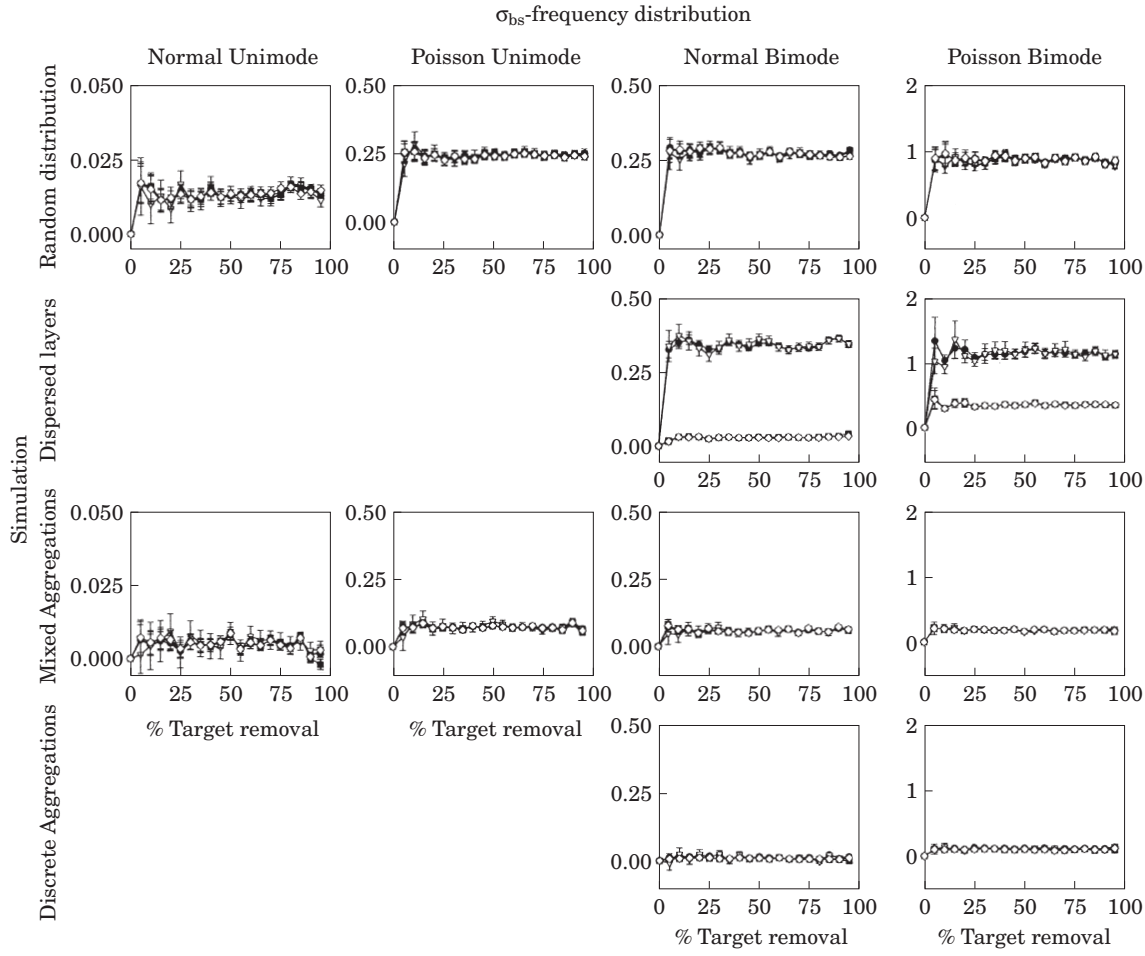

Figure 6. Mean per-capita σ_{bs} deviation index as a function of %target removal. %target removal was incremented in 5% steps. Column comparisons show the effect of using different σ_{bs}-frequency distributions, and row comparisons show the effect on $\hat{\sigma}_{bs}$ estimates using different estimation methods. $\hat{\sigma}_{bs}$ estimation methods are represented by: —●— mean fill, —▽— random fill, —■— local window, and —◇— nearest-neighbor.

with resolved targets were altered to having greater numbers at the mean [vertical bars, Figure 7(a) and (c)]. The local-window and nearest neighbor methods replicated the distribution of σ_{bs}'s rather than the original σ_{bs}-distribution of individual targets throughout the array when σ_{bs}-distributions were random (lower panel, Figure 7). The random-fill method retained the σ_{bs}-distributions of individual targets for all simulation conditions. The mean-fill estimation method altered individual target σ_{bs}-frequency distributions to greatly increase numbers at the mean and reduce the number of $\hat{\sigma}_{bs}$s at intermediate values and tails for all simulation conditions (Figure 7).

Discussion

We recommend the use of a local search window among $\hat{\sigma}_{bs}$ estimation methods examined. The local-window method consistently gave accurate estimates of fish densities and array abundances, and preserved σ_{bs}-frequency distributions. The local-window method combines the nearest-neighbor and mean-fill methods by using the weighted-mean σ_{bs} from a distribution of individual targets in close proximity to cells requiring an estimate of acoustic backscattering cross-section. Using a distribution of individual targets to choose a representative $\hat{\sigma}_{bs}$ reduces the probability of choosing an extreme value when estimating fish density. Since fish tend to aggregate with similar sized individuals of the same species (Ranta and Lindström, 1990; Ranta *et al*., 1992), a local search pattern preserves spatial distributions by using contiguous targets to estimate $\hat{\sigma}_{bs}$. Schooling and shoaling behaviors result in spatially-autocorrelated distributions of fish densities, species, and sizes. In our simulations, estimates of density and abundance were most accurate when spatial distributions of density and

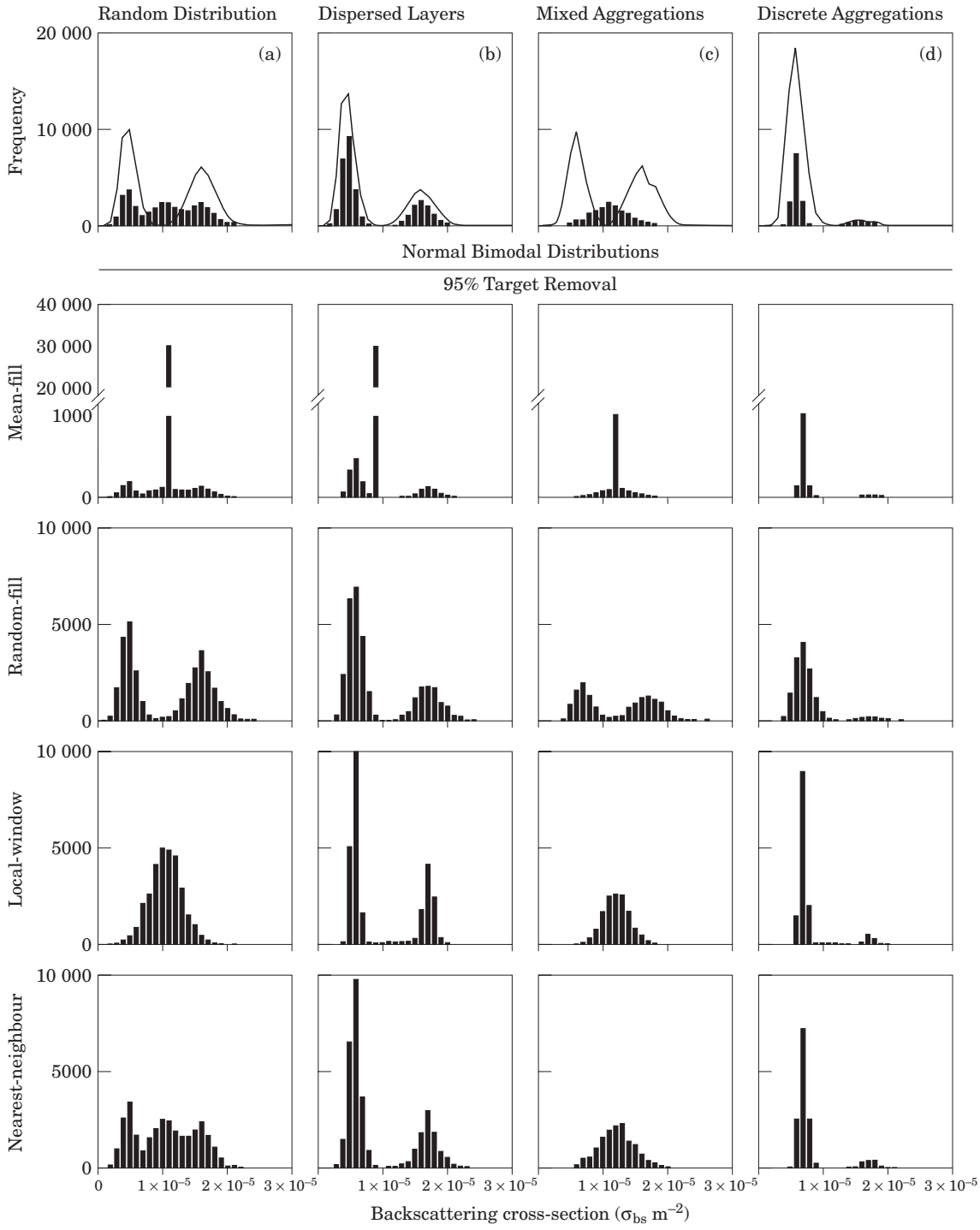

Figure 7. Backscattering cross-section original and simulated frequency distributions after filling cells or target removal. The top panel shows normal bimodal σ_{bs} distributions of individual targets (solid lines) and the resulting σ_{bs} distributions after array cells have been filled and the mean backscattering cross-sections have been calculated (vertical bars). The number of predators (larger σ_{bs} mode) is less in the Discrete Aggregation simulations than in the Random Distribution. The bottom section shows backscattering cross-section distributions in array cells resulting from the four estimation methods after 95% target removal.

backscattering cross-sections were autocorrelated. This is reassuring as spatially-autocorrelated distributions simulate discrete patches of fish typically observed in freshwater, estuarine, and marine environments.

Accuracy of fish density, abundance, and $\hat{\sigma}_{bs}$ estimates declined when as little as 5% of known targets were randomly removed from the data set but did not decrease in proportion to the percentage of known targets removed. Density and σ_{bs} deviation index values remained fairly constant up to 95% target removal, suggesting that backscattering cross-section estimation methods used in this study are not sensitive to the number of available targets. Insensitivity of density, abundance, and $\hat{\sigma}_{bs}$ estimates to numbers of individual targets may be an artifact of randomly removing targets from the entire range of fish sizes. Even at 95% target removal, all modes from multimodal fish size distributions were represented. Subsequent simulations would remove specified size classes in greater proportion to other size classes from multimodal frequency distributions. As an example, prey fish that may not be acoustically resolvable within schools would be separated from predatory species that are resolvable.

Inclusion of backscattering by different types of organisms will reduce the effectiveness of *in situ* targets for density, abundance, and σ_{bs} estimates by increasing the range of, and number of modes in backscattering strength distributions. We simulated spatial distributions of backscattering by organisms of similar acoustic scattering characteristics. Acoustic data collected in the field is comprised of backscatter by a number of physical and biological sources. Behavior and activity levels such as during crepuscular periods when fish vertically and horizontally migrate to feed (Ungar and Brandt, 1989; Levy, 1990, 1991; Boudreau, 1992), will also affect the accuracy of density estimates. Applying volume backscattering and individual target thresholds will reduce the amount of backscattering by non-swimbladdered organisms so that backscatter can be apportioned to swimbladder bearing fish. Varying cell size so that the spatial dimensions of array cells match aggregation dimensions may also increase the utility of *in situ* targets for density and abundance estimates. The strategy used to select representative backscatterers depends on the number of individual targets and the number of species present in a sampling area. Alternatives to using *in situ* targets include using length-frequency distributions from catch data, using species composition and length-frequency distributions from previously collected catch or acoustic data, or changing the time of sampling.

All simulations assume linearity of backscattering (Foote, 1983) from isolated individuals and from individuals within aggregations. Furusawa *et al.* (1992) calculated that attenuation effects on abundance estimates were negligible below packing densities of approximately 0.8 fish m^{-3}. We have not simulated backscattering from the dense schools where non-linear effects on sound transmission such as sound attenuation (Røttingen, 1976) and shadowing (MacLennan and Simmonds, 1992) may be significant. In cases where the summation of backscatter is not linear, algorithms that quantify relationships between acoustic volume backscattering and catch data must be used to ensure accurate density and abundance estimates of fish (Misund *et al.*, 1992) and zooplankton (Hewitt and Demer, 1993). Effects of non-linear sound scattering from densely packed aggregations on fish density and population estimates can be minimized by collecting acoustic data when fish disperse and individual echoes are better resolved (Brandt *et al.*, 1991; Simmonds *et al.*, 1992).

Using *in situ* targets to estimate acoustic backscattering cross-sections within aggregations assumes that species and σ_{bs}-frequency distributions of individual targets match those of non-resolvable individuals within aggregations. This may not always be the case. Rose (1993) found that aggregations of migrating Atlantic cod (*Gadus morhua*) were structured by fish length. When individual targets are not available or not representative of individuals within aggregations, backscattering cross-sections can be estimated using length-frequency data from net catches. Results of catch data–acoustic backscatter comparisons are commonly empirical regression equations describing the relationship between acoustic backscatter and individuals (e.g. Love, 1971; Midttun, 1984; Foote, 1987) or aggregations (e.g. Love, 1975; Rudstam *et al.*, 1987; Fleischer *et al.*, 1997) of fish or zooplankton. Constraints to this approach are that catch data are rarely available from the identical volume surveyed using acoustics, and that catch data are size selective.

In our simulations, as well as when a mean backscattering cross-section is derived from catch data, a distribution of backscattering strengths is characterized as a single value. Wide ranges and/or multimodal distributions of σ_{bs} may not be adequately characterized by a mean. An alternate approach would use the distribution of σ_{bs}'s to form a probability-density-function (PDF) of densities for each array cell. This density PDF may then be used to construct a distribution of population estimates, and potentially for size-based density and abundance estimates.

Quantifying variability in population abundance estimates requires an understanding of the variance at each step in the estimation process. Measurement errors in volume backscattering and variability in individual acoustic backscattering measurements due to fish activity and orientation (e.g. Foote, 1980) or individual echo discrimination (e.g. Demer *et al.*, 1999) occur prior to placing acoustic data into spatial arrays. Variability due to survey or sampling design occurs after cell-based density estimates are made. The goals of these

simulations were to quantify variance in density estimates whilst retaining the spatial complexity of organism distributions. This paper quantified variance associated with selecting a representative acoustic backscattering cross-section from *in situ* targets; extracting spatio-temporal information from acoustic data; and quantifying variability associated with estimates of density and organism size within spatially-indexed cells. In our simulations, the efficacy of backscattering cross-sectional estimation methods was not influenced by measurement or survey design variability. Quantifying variances at each step of the population abundance estimation process allows partitioning of biases incurred when translating acoustic data to biologically and ecologically meaningful metrics.

Acknowledgements

We thank the students (Darryl Hondorp, Dennis Roy, and Lian Zhou) and staff (Karen Barry, Eric Demers, Jiangang Luo, and Jeff Tyler) of the Great Lakes Center SUNY-College at Buffalo, and Lynn Herche of the NOAA-Great Lakes Environmental Laboratory, Ann Arbor, MI for insightful discussions on this problem. We would also like to thank Steve Brandt, Gordie Schwartzman and David Schneider for helpful comments on a presentation of a previous version of this work. Thanks to David Reid (Aberdeen, Scotland), David Demer of the NOAA/NMFS-Southeast Fisheries Science Center, and one anonymous reviewer whose comments clarified this paper. This work was supported by NSF-LMER #032679 (Trophic Interactions in Estuarine Systems) (JMJ), the Office of Naval Research (N00014-89J-1515) (JMJ, JKH), and the New York Sea Grant Institute (NA46RG0090) (JKH). This is GLERL contribution #1203.

References

Boudreau, P. R. 1992. Acoustic observations of patterns of aggregation in haddock (*Melanogrammus aeglefinus*) and their significance to production and catch. Canadian Journal of Fisheries and Aquatic Sciences, 49: 23–31.

Brandt, S. B., and Mason, D. M. 1994. Landscape approaches for assessing spatial patterns in fish foraging and growth. *In* Theory and Application in Fish Feeding Ecology. Ed. by D. J. Stouder, K. L. Fresh, and R. J. Feller. Belle W. Baruch Library in Marine Science, #18.

Brandt, S. B., Mason, D. M., Patrick, E. V., Argyle, R. L., Wells, L., Unger, P. A., and Stewart, D. J. 1991. Acoustic measures of the abundance and size of pelagic planktivores in Lake Michigan. Canadian Journal of Fisheries and Aquatic Sciences, 48: 894–908.

Brandt, S. B., Mason, D. M., and Patrick, E. V. 1992. Spatially-explicit models of fish growth rate. Fisheries, 17: 23–33.

Craig, R. E., and Forbes, S. T. 1969. Design of a sonar for fish counting. Fiskeridirektoratets Skrifter Serie Havundersokelser, 15: 210–219.

Cressie, N. 1991. Statistics for Spatial Data. John Wiley and Sons, Inc., New York.

Demer, D. A., Soule, M. A., and Hewitt, P. R. 1999. A multiple-frequency method for potentially improving the accuracy and precision of *in situ* target strength measurements. Journal of the Acoustical Society of America, 105: 2359–2377.

Dragesund, O., and Olsen, S. 1965. On the possibility of estimating year-class strength by measuring echo-abundance of 0-group fish. Fiskeridirektoratets Skrifter Serie Havundersokelser, 13: 47–75.

Ehrenberg, J. E., and Torkelson, T. C. 1996. Application of dual-beam and split-beam target tracking in fisheries acoustics. ICES Journal of Marine Science, 53: 329–334.

Fleischer, G. W., Argyle, R. L., and Curtis, G. L. 1997. *In situ* relations of target strength to fish size for great lakes pelagic planktivores. Transactions of the American Fisheries Society, 126: 786–794.

Foote, K. G. 1978. Analysis of empirical observations on the scattering of sound by encaged aggregations of fish. Fiskeridirektoratets Skrifter Serie Havundersokelser, 16: 423–456.

Foote, K. G. 1980. Effect of fish behaviour on echo energy: The need for measurements of orientation distributions. Rapports et Process-Verbaux des Réunions du Conseil International pour l'Exploration de la Mer, 39: 193–201.

Foote, K. G. 1983. Linearity of fisheries acoustics, with addition theorems. Journal of the Acoustical Society of America, 73: 1932–1940.

Foote, K. G. 1987. Fish target strengths for use in echo integrator surveys. Journal of the Acoustical Society of America, 82: 981–987.

Foote, K. G., Aglen, A., and Nakken, O. 1986. Measurements of fish target strength with a split-beam echo sounder. Journal of the Acoustical Society of America, 80: 612–621.

Furusawa, M., Ishii, K., and Miyanohana, Y. 1992. Attenuation of sound by schooling fish. Journal of the Acoustical Society of America, 92: 987–994.

Hewitt, R. P., and Demer, D. A. 1993. Dispersion and abundance of Antarctic krill in the vicinity of Elephant Island in the 1992 austral summer. Marine Ecology Progress Series, 99: 29–39.

Horne, J. K., and Schneider, D. C. 1997. Spatial variance of mobile aquatic organisms: capelin and cod in Newfoundland coastal waters. Philosophical Transactions of the Royal Society of London B Biological Sciences, 352: 633–642.

Levy, D. A. 1990. Reciprocal diel vertical migration behavior in planktivores and zooplankton in British Columbia lakes. Canadian Journal of Fisheries and Aquatic Science, 47: 1755–1764.

Levy, D. A. 1991. Acoustic analysis of diel vertical migration behavior of *Mysis relicta* and Kokanee (*Oncorhynchus nerka*) within Okanagan Lake, British Columbia. Canadian Journal of Fisheries and Aquatic Science, 48: 67–72.

Luo, J., and Brandt, S. B. 1993. Bay anchovy *Anchoa mitchelli* production and consumption in mid-Chesapeake Bay based on a bioenergetics model and acoustic measures of fish abundance. Marine Ecological Progress Series, 98: 223–236.

Love, R. H. 1971. Measurements of fish target strengths: A review. Fisheries Bulletin, 69: 703–715.

Love, R. H. 1975. Predictions of volume scattering strengths from biological trawl data. Journal of the Acoustical Society of America, 57: 300–305.

MacLennan, D. N., and Simmons, E. J. 1992. Fisheries Acoustics. Chapman and Hall, London. 325 pp.

Mason, D. M., and Brandt, S. B. 1996. Effects of spatial scale and foraging efficiency on the predictions made by spatially-explicit models of fish growth rate potential. Environmental Biology of Fishes, 45: 283–298.

Medwin, H., and Clay, C. S. 1997. Fundamentals of Acoustical Oceanography. Academic Press, NY. 712 pp.

Megard, R. O., Kuns, M. M., Whiteside, M. C., and Downing, J. A. 1997. Spatial distributions of zooplankton during coastal upwelling in western Lake Superior. Limnology and Oceanography, 42: 827–840.

Midttun, L. 1984. Fish and other organisms as acoustic targets. Rapports et Process-Verbaux des Réunions du Conseil International pour l'Exploration de la Mer, 184: 25–33.

Misund, O. A., Aglen, A., Beltestad, A. K., and Dalen, J. 1992. Relationships between the geometric dimensions and biomass of schools. ICES Journal of Marine Science, 49: 305–315.

Nash, R. D. M., Magnuson, J. J., Stanton, T. K., and Clay, C. S. 1989. Distribution of peaks of 70 kHz acoustic scattering in relation to depth and temperature during day and night at the edge of the Gulf Stream-EchoFront 83. Deep-Sea Research, 36: 587–596.

Petitgas, P. 1993. Geostatistics for fish stock assessments: a review and an acoustic application. ICES Journal of Marine Science, 50: 285–298.

Ranta, E., and Lindström, K. 1990. Assortative schooling in three-spined sticklebacks? Annuales Zoologici Fennici, 27: 67–75.

Ranta, E., Lindström, K., and Peuhkuri, N. 1992. Size matters when three-spined sticklebacks go to school. Animal Behaviour, 43: 160–162.

Rose, G. A. 1993. Cod spawning on a migration highway in the north-west Atlantic. Nature, 366: 458–461.

Røttingen, I. 1976. On the relation between echo intensity and fish density. Fiskeridirektoratets Skrifter Serie Havundersokelser, 16: 301–314.

Rudstam, L. G., Clay, G. S., and Magnuson, J. J. 1987. Density and size estimates of cisco, Coregonus artedii using analysis of echo peak PDF froma single transducer sonar. Canadian Journal of Fisheries and Aquatic Science, 44: 811–821.

Simmonds, E. J., and Fryer, R. J. 1996. Which are better, random or systematic acoustic surveys? A simulation using North Sea herring as an example. ICES Journal of Marine Science, 53: 39–50.

Simmonds, E. J., Williamson, N. J., Gerlotto, F., and Aglen, A. 1992. Acoustic survey design and analysis procedure: a comprehensive review of current practice. ICES Cooperative Research Report #187, Copenhagen, Denmark. 128 pp.

Soule, M. A., Hampton, I., and Barange, M. 1996. Potential improvements to current methods of recognizing single targets with split-beam echo-sounder. ICES Journal of Marine Science, 53: 237–244.

Unger, P. A., and Brandt, S. B. 1989. Seasonal and diel changes in sampling conditions for acoustic surveys of fish abundance in small lakes. Fisheries Research, 7: 353–366.